Surface Science 707 (2021) 121785

Contents lists available at ScienceDirect

Surface Science

journal homepage: www.elsevier.com/locate/susc

Highly sensitive detection of H_2O adsorbed on Si(111)7 × 7 and Si(100)2 × 1 surfaces by means of slow highly charged Xe ions

Satoshi Takahashi [*,a], Masahide Tona [b], Nobuyuki Nakamura [a], Chikashi Yamada [a], Makoto Sakurai [c], Shunsuke Ohtani [a]

[a] The University of Electro-Communications, Chofu, Tokyo 182-8585, Japan
[b] Ayabo Corporation, 1 Fukamacho Hosogute, Anjo-shi, Aichi 446-0052, Japan
[c] Department of Physics, Kobe University, Hyogo 657-8501, Japan

ARTICLE INFO

Keywords:
Highly charged ion
Potential sputtering
Proton sputtering
Water
Silicon
Secondary-ion mass spectrometry
2010 MSC:
00-01
99-00

ABSTRACT

The proton yields from Si(111)7 × 7 and Si(100)2 × 1 reconstructed surfaces irradiated with slow ($v < 0.25v_{Bohr}$) highly charged Xe ions are obtained. H_2O molecules adsorbed over time on the surfaces at room temperature, under ultra-high vacuum can be detected as an increase of the proton yield. For the Si(100)2 × 1 surface, the proton yield with HCI-irradiation time is discussed based on temporal variation of the H_2O coverage. The proton desorption efficiency with Xe^{50+} is more than about ten times and twice as compared with Xe^{29+} and Xe^{44+}, respectively. For the Si(111)7 × 7 and Si(100)2 × 1 surfaces, the proton yield in each time increases with the charge states q to the power of 6 and 4, respectively, and is changed with time with the power laws held on.

1. Introduction

A highly charged ion (HCI) has a large potential energy, E_p, which is the summation of the ionization energies obtained by removing electrons from a neutral atom. Being slower than the electrons in a solid ($< 10^6$m/s), when a HCI approaches a solid surface, electrons move from the surface to the HCI within a few femtoseconds, which is shorter than the time period during which the HCI interacts with the surface. The HCI then releases most of its E_p resulting in the emission of secondary electrons, ions, neutrals, and photons caused by capturing electrons from the surface. The emission mechanism of secondary ions and neutrals, which is known as potential sputtering, differs from that due to kinetic sputtering [1–3]. With HCI irradiation, protons are emitted as typical secondary ions when hydrogen species (e.g., H_2, H_2O, or other hydride molecules) have been adsorbed either physically or chemically as impurities on the material. Proton desorption is caused by Coulomb repulsion between a proton and an adjacent ion after giving out two electrons from a chemical bond of hydrogen (pair-wise potential sputtering (PWPS) [4]). The proton yield increases with the charge state, q, to the power of 3–6 [5–8].

Proton desorption depends on surface chemical property. For example, in the case of gold surfaces covered with a surfactant monolayer (ML), the proton yield from carboxyl group of mercaptoundecanoic acid ($HS(CH_2)_{10}COOH$) is larger than that from methyl group of dodecanethiol ($HS(CH_2)_{11}CH_3$). A hydrogen atom in the carboxyl group is easily desorbed as compared with that in the methyl group. In the process of HCI capturing two bonding electrons from a chemical bond, the hydrogen atom is more easily ionized as a proton from OH bond than from CH bond, because the electronegativity of oxygen is higher than that of carbon [9]. A HCI captures electrons into its outer shells. In case of the fluorine adsorbed on Si(100)2 × 1 surface, the angular distribution of F^+ ion has been observed. The desorbed F^+ ion image indicates the bond direction and angle between F and Si on the surface. Above the surface, a HCI captures electrons from a chemical bond of F–Si into its high Rydberg states, and desorbs F without destroying surface structure before colliding with the surface [10].

In this study, we focus on clean reconstructed Si surfaces that contain almost no hydrogen. The structure of a reconstructed Si surface after being cleaned at 1500 K differs from that of the bulk. In a Si(100) surface, a Si atom on the surface has two dangling bonds and approaches an adjacent Si atom, where the two atoms bond to form a 2 × 1 Si dimer [11]. The remaining single dangling bonds of the Si atoms remain on the

* Corresponding author.
E-mail address: satoshi@ils.uec.ac.jp (S. Takahashi).

https://doi.org/10.1016/j.susc.2020.121785
Received 9 July 2020; Received in revised form 13 November 2020; Accepted 17 December 2020
Available online 24 December 2020

surface and are exposed by the residual gas, under ultra-high vacuum (UHV). Dissociative adsorption of H_2O, which is one of the main constituents of the residual gas, occurs on the surface [12]. The H_2O coverage depending on the flux of H_2O molecules changes constantly until saturation and have been obtained using temperature-programmed desorption (TPD) [13]. In the case of a Si(111) surface, the structure of a Si(111)7 × 7 surface, called the dimer adatom stacking-fault model, is reconstructed to from the top layer to the third layer of the surface [14]. As there are 19 dangling bonds in the 7 × 7 unit cell, dissociative adsorption of H_2O occurs on the surface similar to that of a Si(100)2 × 1 surface [12].

In this paper, we show that the high q-HCIs (up to q=50) usefully act as the ultra-sensitive probe for the investigation into the initial stage of the hydrogen-adsorption process, which is a development from previous work [15].

2. Experimental details

HCIs were produced at the University of Electro-Communications in an electron-beam ion trap (EBIT) known as the Tokyo EBIT [16], where they were transported to a collision chamber using a beamline [17]. The HCIs had a kinetic energy $E_k = 3.5q$ keV owing to the acceleration voltages 3 kV and − 0.5 kV that were applied to the drift tube in the EBIT and to a sample, respectively. The collision chamber was equipped with an instrument for time-of-flight secondary ion mass spectrometry (TOF-SIMS) and a low-energy electron diffraction (LEED) apparatus, where the base pressure was 4.0×10^{-8} Pa. The partial pressure of the residual gas was obtained using a quadrupole mass spectrometer, the main constituents of the residual gas at the base pressure were estimated as 35% H_2, 31% H_2O, 25% CO and negligible CO_2.

The TOF-SIMS setup has been described elsewhere [8]. Secondary ions were detected with a micro-channel plate (MCP) detector with a resistive anode, i.e., a position sensitive detector (PSD). It was confirmed that secondary ions were collected within the active area of the PSD with cylindrical electrostatic lenses; trajectories of proton were simulated using SIMION 3D software [18], and every trajectory ended in the active area for the protons having less than 25 eV. Protons are dominantly emitted within a few tens eV due to potential sputtering [6]. Therefore, the errors of collection efficiency of secondary ions in this TOF-SIMS instrument is 98.1 ± 0.5% negligible compared with others. Three meshes were attached to the TOF tube and lenses. The transmission efficiency of secondary ions passing through the meshes was 48.5 ± 0.5%, as estimated from the open-area ratio of the mesh. The detection efficiency of the MCP for 1.5-keV H^+ was assumed to be 60.5 ± 5%, after Gao et al. [19]. Considering these factors, the absolute efficiency was determined to be $\eta = 28.8 \pm 1.8\%$. The secondary ion counts and yields measured in this work were corrected by dividing by η.

Si(111) and Si(100) samples were cut into 5 mm × 20 mm size from 0.5-mm-thick Si(111) and Si(100) n-type wafers with resistivities of 10 and 1 Ωcm, respectively. The samples were cleaned ultrasonically in (i) acetone for 10 min and (ii) wash fluid (Semico Clean 23; Furuuchi Chemical Co., Ltd., Japan) for 10 min and then rinsed in ultra-pure water (> 18 MΩcm). The samples were heated in situ at 750 K to degas them and their holders under UHV until the pressure had stabilized near the base pressure for at least 10 h. The samples were flashed repeatedly at 1500 K by resistive heating and were cooled slowly, at rates of less than 2 K/s, from 1200 K to room temperature [20]. The Si(111)7 × 7 and Si (100)2 × 1 structures were confirmed from their LEED patterns, and no contamination was detected within the sensitivity of Auger electron spectroscopy (AES).

Most of the Si(111)7 × 7 and Si(100)2 × 1 samples were irradiated with Xe^{q+} (q=29, 38, 44, 47 and 50); however, one of the Si(100)2 × 1 samples was not irradiated with Xe^{47+}. The intensity of the Xe HCI beam through a 1-mm-diameter aperture was less than 1700/s. The surface normal of the samples was oriented so that the angle of incidence of the Xe HCI beam was 60°. The filament of the ionization gauge was switched off to avoid generation of atomic hydrogen whose sticking probability is higher than that of H_2. The samples were flashed at 1500 K for a few seconds before being irradiated with Xe HCIs. The TOF-SIMS measurement was recorded immediately after sample flashing; this was done to obtain the proton yield that was proportional to the amount of H_2O adsorbed on the surface, which in turn increased with time. In this paper, time indicates HCI-irradiation time from a started record of TOF-SIMS measurement cycle.

3. Results and discussion

Fig. 1 shows the TOF spectra from Si(111)7 × 7 surfaces irradiated with Xe HCIs at 2.5 min after sample flashing. The peaks are identified as photons, H^+, H_2^+ and Si^{n+} ($n \leq 4$). The intensity of H^+ from the Si(111)7 × 7 surface irradiated with Xe^{50+} was one order of magnitude smaller than that from a hydrogen-terminated Si(111)1 × 1 surface in previous work [8]. The peaks of Si^{n+} are obviously shaped with the charge state q. The each yield of Si^{n+} increases with the charge state q to the power of 2, and are affected by potential sputtering, since the yields of H^+, Si^+ and Si^{2+} from a hydrogen-terminated Si(111)1 × 1 surface is almost independent of kinetic energy of HCIs in the energy range of 119–257 keV [21]. Si^{n+} ions produced by HCI capturing electrons acquires desorption momentum of Si atom by Coulomb repulsion force between Si^{n+} ions. Fig. 2 shows the TOF spectra from a Si(111)7 × 7 surface irradiated with Xe^{50+} at 20 and 140 min after sample flashing. At the later time, the intensity of H^+ had increased drastically and those of O^+ and O^{2+} had increased only slightly, which is clear evidence for the dissociative adsorption of H_2O.

Fig. 3 (a) and (b) show the proton yields $Y_{H^+}^{(111)}$ and $Y_{H^+}^{(100)}$ from Si (111)7 × 7 and Si(100)2 × 1 surfaces obtained in 20 and 45 min, respectively, after sample flashing. Each value of $Y_{H^+}^{(111)}$ and $Y_{H^+}^{(100)}$ is a 5-min average, which increased linearly with time after sample flashing, and increased with the charge state q. The intersections of the proton yields with the horizontal-axis are −20 to −28 and −5 to −10 min, respectively. In Fig. 3(b), H_2O adsorbption on the surface from 800 K to room temperature occurs for several min. In Fig. 3(a), it is considered that adsorbed H_2O have slightly been remaining on the surface after sample flashing because of insufficient flashing time. The increase in the amount of H_2O adsorbed on the surfaces could be detected as increases of $Y_{H^+}^{(111)}$ and $Y_{H^+}^{(100)}$. Increases per min of proton yield, namely $dY_{H^+}^{(111)}/dt$ and $dY_{H^+}^{(100)}/dt$, are given in Table 1.

Fig. 4 (a) and (b) show charge state dependence of proton yield from Si(111)7 × 7 and Si(100)2 × 1 surfaces in each time after sample flashing. The proton yields in Fig. 4(a) and (b) are translated from those in Fig. 3(a) and (b), respectively. For Si(111)7 × 7 and Si(100)2 × 1 surfaces, the proton yield in each time increases with the charge state q to the power of 6 and 4, respectively. The power law are applied to the

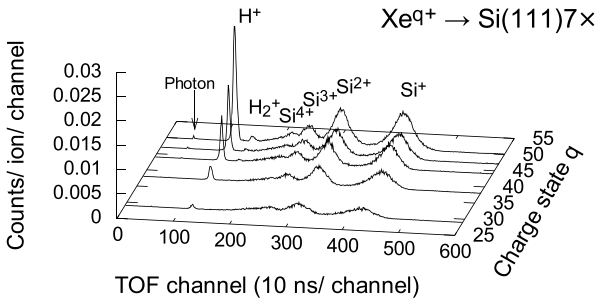

Fig. 1. Time-of-flight spectra from Si(111)7 × 7 surfaces irradiated with 3.5q-keV Xe^{q+} (q=29, 38, 44, 47 and 50) at 2.5 min after sample flashing.

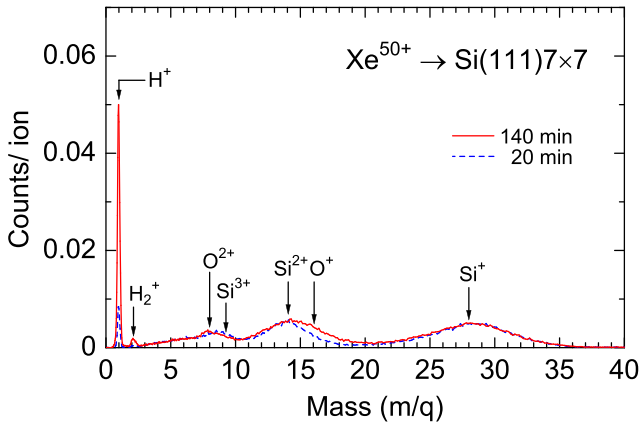

Fig. 2. Mass spectra from a Si(111)7 × 7 surface irradiated with 175-keV Xe^{50+}. The dashed (blue) and solid (red) line represent the mass spectra at 20 and 140 min, respectively, after sample flashing.

Table 1
For Si(111)7 × 7 and Si(100)2 × 1 surfaces, increases per min of proton yield, and ratios of differential of proton yield to that of H_2O coverage.

q	$dY_{H^+}^{(111)}/dt \times 10^{-3}$ (/ion min)	$dY_{H^+}^{(100)}/dt \times 10^{-3}$ (/ion min)	$dY_{H^+}^{(100)}/d\theta_{H_2O}^{(100)}$ (/ion ML)
50	6.0 ± 0.4	8.6 ± 0.5	2.8 ± 0.6
44	2.6 ± 0.2	4.1 ± 0.3	1.3 ± 0.3
38	1.1 ± 0.1	1.8 ± 0.1	0.58 ± 0.12
29	0.50 ± 0.03	1.0 ± 0.1	0.32 ± 0.07

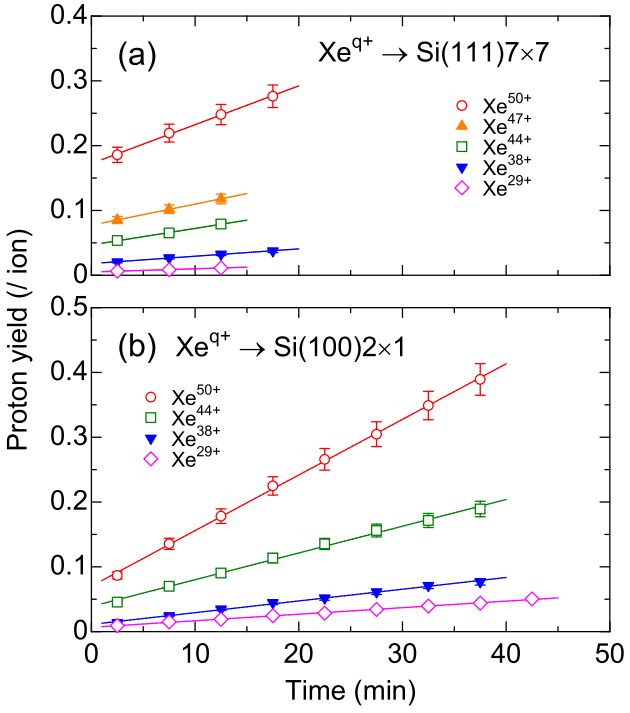

Fig. 3. Proton yields from (a) Si(111)7 × 7 surfaces and (b) Si(100)2 × 1 surfaces irradiated with Xe HCIs versus time after sample flashing. The open circles (red), solid triangles (orange), open squares (green), solid upside-down triangles (blue) and open diamonds (pink) represent the proton yields for Xe^{50+}, Xe^{47+}, Xe^{44+}, Xe^{38+} and Xe^{29+}, respectively.

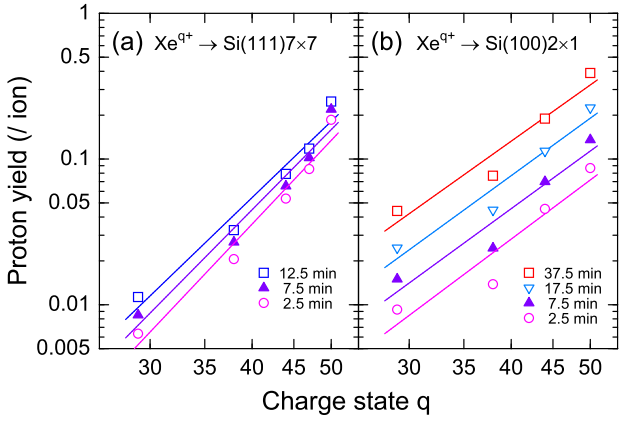

Fig. 4. Charge state dependence of proton yield from (a) Si(111)7 × 7 surfaces and (b) Si(100)2 × 1 surfaces in each time after sample flashing. Proton yields of (a) and (b) are translated from those in Fig. 3(a) and (b), respectively. For each value, the error is within ±6–9%. The open circles (pink), solid triangles (purple), open squares (blue), open upside-down triangles (light blue) and open squares (red) represent the proton yields at 2.5, 7.5, 12.5, 17.5 and 37.5 min, respectively, after sample flashing.

PWPS model predicted in lower charge states ($q \leq 10$) [4]. With the power law q^6 and q^4 held on, the proton yields are changed with time. The power law depends on not time but the charge state q.

In the case of a Si(100)2 × 1 surface, we deduce that H_2O is preferentially adsorbed on the surface for the following two reasons. (1) The sticking probability of H_2O on the surface at room temperature is unity, which is sufficiently higher than those of the other residual-gas components H_2, CO, and CO_2 [22,23]. (2) The impinging rate of H_2O is estimated to be $P/\sqrt{2\pi m k_B T} \simeq (3.6 \pm 0.7) \times 10^{14}/m^2s$, where P estimated as the partial pressure of H_2O at the base pressure was $(1.0 \pm 0.2) \times 10^{-8}$ Pa, m is the H_2O mass, k_B is the Boltzmann constant, and T is 300 K (room temperature), and is large enough compared with that of incident Xe HCIs, which is estimated as being less than $2.2 \times 10^9/m^2s$. This indicates that Xe HCIs do not prevent H_2O from adsorption on the surface. In TOF-SIMS measurement, it must be emphasized that surface damage in the case of HCI irradiation is extremely little as compared with that in the case of singly charged ion of which the intensity, e.g., a few nA, is seven orders of magnitude larger than that of HCI. The H_2O coverage, $\theta_{H_2O}^{(100)}$, is ideally half a ML in saturation, where the surface is fully terminated by –H and –OH. In this HCI-SIMS experiment, we define the proton desorption efficiency to be the ratio of $dY_{H^+}^{(100)}/dt$ to the H_2O adsorption rate, namely $d\theta_{H_2O}^{(100)}/dt$. The proton desorption efficiency needs to consider as the average efficiency of proton desorption from Si–OH and Si–H. Fig. 5 shows the $Y_{H^+}^{(100)}$ obtained in this work with Xe^{50+} (open circles). The intersection of the proton yields with the horizontal-axis in Fig. 3(b) is corrected to 0 min. The $Y_{H^+}^{(100)}$ is compared with the H_2O adsorption rate (solid line) calculated from the sticking probability of H_2O at unity and the partial pressure of H_2O. The H_2O adsorption rate is estimated to be $(3.1 \pm 0.6) \times 10^{-3}$ ML/min. The proton desorption efficiency, namely $dY_{H^+}^{(100)}/d\theta_{H_2O}^{(100)}$, was calculated as given in table 1. These results show a remarkable increase of the proton desorption efficiency with the charge state q. For example, the proton desorption efficiency with Xe^{50+} is more than about ten times and twice as compared with Xe^{29+} and Xe^{44+}, respectively.

4. Conclusion

With Xe HCI irradiation, the proton yields increase with increasing

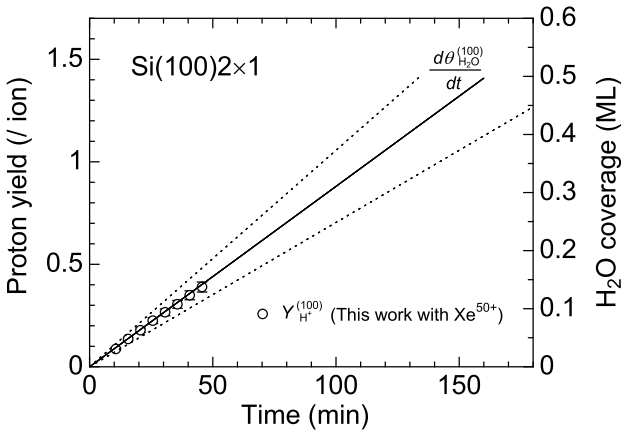

Fig. 5. The proton yields (open circles) from the Si(100)2 × 1 surface irradiated with Xe^{50+} versus time. The intersection of the proton yields with the horizontal-axis in Fig. 3(b) is corrected to 0 min. The solid and dotted lines represent the H_2O coverage, which is calculated from the sticking probability of H_2O at unity and the partial pressure of H_2O at $(1.0 \pm 0.2) \times 10^{-8}$ Pa, and minimum and maximum errors of the H_2O coverage.

the amount of H_2O adsorbed on Si(111)7 × 7 and Si(100)2 × 1 surfaces over time after sample flashing. In particular, the proton desorption efficiency as derived from $dY_{H^+}^{(100)}/d\theta_{H_2O}^{(100)}$ for the Si(100)2 × 1 surface with Xe^{50+} is 3.5 ± 1.1 /ion ML, and is more than about ten times and twice as compared with Xe^{29+} and Xe^{44+}, respectively. For the Si(111)7 × 7 and Si(100)2 × 1 surfaces, the proton yield in each time increases with the charge state q to the power of 6 and 4, respectively, and is changed with time with the power laws held on. The power law depend on not time but the charge state q. The proton desorption efficiency indicates the power law q^6 and q^4, respectively. A high q-HCI is a highly sensitive probe for hydrogen on various materials.

CRediT authorship contribution statement

Satoshi Takahashi: Investigation, Writing - original draft. **Masahide Tona:** Investigation, Writing - review & editing. **Nobuyuki Nakamura:** Conceptualization, Writing - review & editing. **Chikashi Yamada:** Conceptualization, Writing - review & editing. **Makoto Sakurai:** Conceptualization, Writing - review & editing. **Shunsuke Ohtani:** Supervision.

Declaration of Competing Interest

The authors declare that they have no known competing financial interests or personal relationships that could have appeared to influence the work reported in this paper.

Acknowledgments

The authors would like to thank Dr. Kazuo Nagata for his help in Si sample preparation and analysis. This work was supported by the CREST program “Creation of Ultrafast, Ultralow Power, Super-performance Nanodevices and Systems” of the Japan Science and Technology Agency and was part of the activity of the 21st Century Center of Excellence (COE) Program “Innovation in Coherent Optical Science” of the University of Electro-Communications.

References

[1] A. Arnau, F. Aumayr, P.M. Echenique, M. Grether, W. Heiland, J. Limburg, R. Morgenstern, P. Roncin, S. Schippers, R. Schuch, N. Stolterfoht, P. Varga, T.J. M. Zouros, H.P. Winter, Interaction of slow multicharged ions with solid surfaces, Surf. Sci. Rep. 27 (1997) 113–239, https://doi.org/10.1016/S0167-5729(97)00002-2.

[2] T. Schenkel, A.V. Hamza, A.V. Barnes, D.H. Schneider, Interaction of slow, very highly charged ions with surfaces, Prog. Surf. Sci. 61 (1999) 23–84, https://doi.org/10.1016/S0079-6816(99)00009-X.

[3] The Physics of Multiply and Highly Charged Ions: Volume 2: Interaction with Matter, in: F.J. Currell (Ed.), Springer, 2003, https://doi.org/10.1007/978-94-017-0544-8.

[4] J. Burgdörfer, Y. Yamazaki, Above-surface potential sputtering of protons by highly charged ions, Phys. Rev. A 54 (1996) 4140–4144, https://doi.org/10.1103/PhysRevA.54.4140.

[5] S. Della-Negra, J. Depauw, H. Joret, Y. Le Beyec, E.A. Schweikert, Secondary ion emission induced by multicharged 18-keVion bombardment of solid targets, Phys. Rev. Lett. 60 (1988) 948–951, https://doi.org/10.1103/PhysRevLett.60.948.

[6] N. Kakutani, T. Azuma, Y. Yamazaki, K. Komaki, K. Kuroki, Potential sputtering of protons from a surface under slow highly charged ion bombardment, Jpn. J. Appl. Phys. 34 (1995) L580–L583, https://doi.org/10.1143/jjap.34.l580.

[7] K. Kuroki, N. Okabayashi, H. Torii, K. Komaki, Y. Yamazaki, Potential sputtering of proton from hydrogen-terminated Si(100) surfaces induced with slow highly charged ions, Appl. Phys. Lett. 81 (2002) 3561–3563, https://doi.org/10.1063/1.1520335.

[8] S. Takahashi, M. Tona, K. Nagata, N. Nakamura, N. Yoshiyasu, C. Yamada, S. Ohtani, M. Sakurai, Toward over unity proton sputtering yields from a hydrogen-terminated si(111) 1 × 1 surface irradiated by slow highly charged xe ions, Appl. Phys. Lett. 87 (2005) 063111, https://doi.org/10.1063/1.2009829.

[9] M. Flores, B.E. O'Rourke, Y. Yamazaki, V.A. Esaulov, Potential and kinetic sputtering of alkanethiol self-assembled monolayers by impact of highly charged ions, Phys. Rev. A 79 (2009) 022902, https://doi.org/10.1103/PhysRevA.79.022902.

[10] N. Okabayashi, K. Komaki, Y. Yamazaki, Enhanced sputtering from the **F**/Si(100) surface with extraction of the surface bond direction, Phys. Rev. Lett. 107 (2011) 113201, https://doi.org/10.1103/PhysRevLett.107.113201.

[11] R.M. Tromp, R.J. Hamers, J.E. Demuth, Si(001) dimer structure observed with scanning tunneling microscopy, Phys. Rev. Lett. 55 (1985) 1303–1306, https://doi.org/10.1103/PhysRevLett.55.1303.

[12] H. Ibach, H. Wagner, D. Bruchmann, Dissociative chemisorption of h_2o on si(100) and si(111) - a vibrational study, Solid State Commun. 42 (1982) 457–459, https://doi.org/10.1016/0038-1098(82)90972-3.

[13] M. C. Flowers, N.B.H. Jonathan, A. Morris, S. Wright, The adsorption and reactions of water on si(100)-2 × 1 and si(111)-7 × 7 surfaces, Surf. Sci. 351 (1996) 87–102, https://doi.org/10.1016/0039-6028(95)01299-0.

[14] K. Takayanagi, Y. Tanishiro, S. Takahashi, M. Takahashi, Structure analysis of si (111)-7 × 7 reconstructed surface by transmission electron diffraction, Surf. Sci. 164 (1985) 367–392, https://doi.org/10.1016/0039-6028(85)90753-8.

[15] S. Takahashi, K. Nagata, M. Tona, M. Sakurai, N. Nakamura, C. Yamada, S. Ohtani, Diet in highly charged ion interaction with silicon surfaces, Surf. Sci. 593 (2005) 318–323, https://doi.org/10.1016/j.susc.2005.06.077.

[16] F. Currell, J. Asada, K. Ishii, A. Minoh, K. Motohashi, N. Nakamura, K. Nishizawa, S. Ohtani, K. Okazaki, M. Sakurai, H. Shiraishi, S. Tsurubuchi, H. Watanabe, A new versatile electron-beam ion trap, J. Phys. Soc. Jpn. 65 (1996) 3186–3192, https://doi.org/10.1143/JPSJ.65.3186.

[17] H. Shimizu, F.J. Currell, S. Ohtani, E.J. Sokell, C. Yamada, T. Hirayama, M. Sakurai, Characteristics of the beam line at the tokyo electron beam ion trap, Rev. Sci. Instrum. 71 (2000) 681–683, https://doi.org/10.1063/1.1150259.

[18] D.A. Dahl, SIMION 3D version 7.0, Idaho National Engineering and Environmental Laboratory.

[19] R.S. Gao, P.S. Gibner, J.H. Newman, K.A. Smith, R.F. Stebbings, Absolute and angular efficiencies of a microchannel-plate position-sensitive detector, Rev. Sci. Instrum. 55 (1984) 1756–1759, https://doi.org/10.1063/1.1137671.

[20] B.S. Swartzentruber, Y.-W. Mo, M.B. Webb, M.G. Lagally, Scanning tunneling microscopy studies of structural disorder and steps on Si surfaces, J. Vac. Sci. Technol. A 7 (1989) 2901–2905, https://doi.org/10.1116/1.576167.

[21] M. Tona, K. Nagata, S. Takahashi, N. Nakamura, N. Yoshiyasu, M. Sakurai, C. Yamada, S. Ohtani, Some characteristics in the interaction of slow highly charged iq+ ions with a si(111) 1 × 1-h surface, Surf. Sci. 600 (2006) 124–132, https://doi.org/10.1016/j.susc.2005.10.020.

[22] B.A. Joyce, J.H. Neave, Electron beam-adsorbate interactions on silicon surfaces, Surf. Sci. 34 (1973) 401–419, https://doi.org/10.1016/0039-6028(73)90126-X.

[23] D. Schmeisser, A comparative study of o_2, h_2 and h2o adsorption on si(100), Surf. Sci. 137 (1984) 197–210, https://doi.org/10.1016/0039-6028(84)90685-X.